Wetlands Ecol Manage
https://doi.org/10.1007/s11273-023-09919-2

ORIGINAL PAPER

Wetland mapping at 10 m resolution reveals fragmentation in southern Nigeria

Sani Idris Garba · Susanna K. Ebmeier · Jean-François Bastin · Danilo Mollicone · Joseph Holden

Received: 11 March 2022 / Accepted: 3 March 2023
© The Author(s) 2023

Abstract Wetland ecosystems play key roles in global biogeochemical cycling, but their spatial extent and connectivity is often not well known. Here, we detect the spatial coverage and type of wetlands at 10 m resolution across southern Nigeria (total area: 147,094 km^2), thought to be one of the most wetland-rich areas of Africa. We use Sentinel-1 and Sentinel-2 imagery supported by 1500 control points for algorithm training and validation. We estimate that the swamps, marshes, mangroves, and shallow water wetlands of southern Nigeria cover 29,924 km^2 with 2% uncertainty of 460 km^2. We found larger mangrove and smaller marsh extent than suggested by earlier, coarser spatial resolution studies. Average continuous wetland patch areas were 120, 11, 55 and 13 km^2 for mangrove, marsh, swamp, and shallow water respectively. Our final map with 10 m pixels captures small patches of wetland which may not have been observed in earlier mapping exercises, with 20% of wetland patches being < 1 km^2; these were clustered around urban centres, suggesting anthropogenic wetland fragmentation. Our approach fills a knowledge gap between very local (< 400 km^2) studies reliant on field studies and aerial photos, and low resolution (> 250 m pixel dimensions) global wetland datasets and provides data critical for both improving land-surface climate models and for wetland conservation.

Keywords Swamp · Marsh · Mangrove · Optical indices · SAR polarimetric indices · Random forest · Uncertainty

Introduction

Wetlands are one of the world's most important and productive ecosystem types, playing a vital role in climate change mitigation (Hassan et al. 2014), hydrological and biogeochemical cycles (Junk et al. 2013) and maintaining livelihoods (Hu et al. 2017; Wilen & Bates 1995). The southern part of Nigeria contains many wetlands which are thought to consist mainly of marshes, mangroves and freshwater swamps (Ayanlade & Proske 2016; Olalekan et al. 2014). However, great environmental pressure has been exerted on these ecosystems as result of land reclamation for agriculture and industrialization (e.g., Niger delta; Chidumeje et al. 2015), urbanization (e.g., Lekki

S. I. Garba (✉) · J. Holden
water@leeds, School of Geography, University of Leeds, Leeds LS2 9JT, UK
e-mail: gysig@leeds.ac.uk

S. K. Ebmeier
School of Earth and Environment, University of Leeds, Leeds LS2 9JT, UK

J.-F. Bastin
TERRA, Teaching and Research Centre, Gembloux Agro Bio-Tech, Université de Liège, Liège, Belgium

D. Mollicone
Food and Agriculture Organization of the United Nations, Rome, Italy

Published online: 31 March 2023

lagoon of Lagos; Obiefuna et al. 2013) and contamination from pollution (e.g., oil spills; Igu & Marchant 2017; Ohimain 1996). The regional extent of existing wetlands that need protecting, and the extent of wetland loss and degradation, has thus far only been quantified at coarse resolution. Although there are some global wetland maps, such as Global Land Cover GLC250-2010 (250 m pixels) and the Global Lakes and Wetlands Database (GLWD-3, 1 km pixels), studies by Gumbricht et al. (2017), Hu et al. (2017) and Xu et al. (2018) show inconsistencies between them due to differences in methods, data sources, and validation. Many global wetland maps rely on data that can be decades old and, particularly in developing countries, with very limited ground truth data. It is therefore important to improve maps of these ecosystems, using a range of techniques, to get a complete picture of wetland area and to establish the range and extent of different wetland types and their fragmentation. Comprehensive wetland maps and an understanding of the nature of their fragmentation are needed to build economic assessments of wetland ecosystem service provision and to support decision-making by regional and international bodies seeking to protect wetland systems as well as for inclusion in coupled land-surface—climatic models (e.g., JULES/QUEST: Clark et al. 2011; Dadson et al. 2010). The latter is crucial since wetlands are important for land–atmosphere carbon dynamics, greenhouse gas exchange, and the water cycle.

Southern Nigeria is a low-lying region covering ~ 147,094 km^2 (between 4° 00′ and 7° 00′N, and 3° 00′ and 9° 00′E, Fig. 1) and is thought to have the most extensive wetlands in west Africa (Gumbricht et al. 2017; Uloacha & Okeke 2004, 2004). However, this area is undergoing huge population expansion and development and so the wetlands may be at risk. The only wetland maps that currently span all of southern Nigeria are from global projects (e.g., GLWD-3) and have relatively low resolution (1 km). However, there are some small-scale studies that have mapped a few small areas of wetland in the region using satellite imagery (e.g., Ayanlade & Proske 2016; Obiefuna et al. 2013; Taiwo & Areola 2009; locations shown in Fig. 1). The accuracy of these small-scale studies has yet to be assessed due to absence of suitable ground truthing data. Furthermore, the techniques used in these studies are not suitable for larger region or country-scale wetland mapping.

Satellite images have been used successfully to identify and map different wetland types around the world (Fei et al. 2011; Guo et al. 2017; Klemas 2011; Kuenzer et al. 2011; Mahdianpari et al. 2018). Interpretation of multi-temporal imagery in

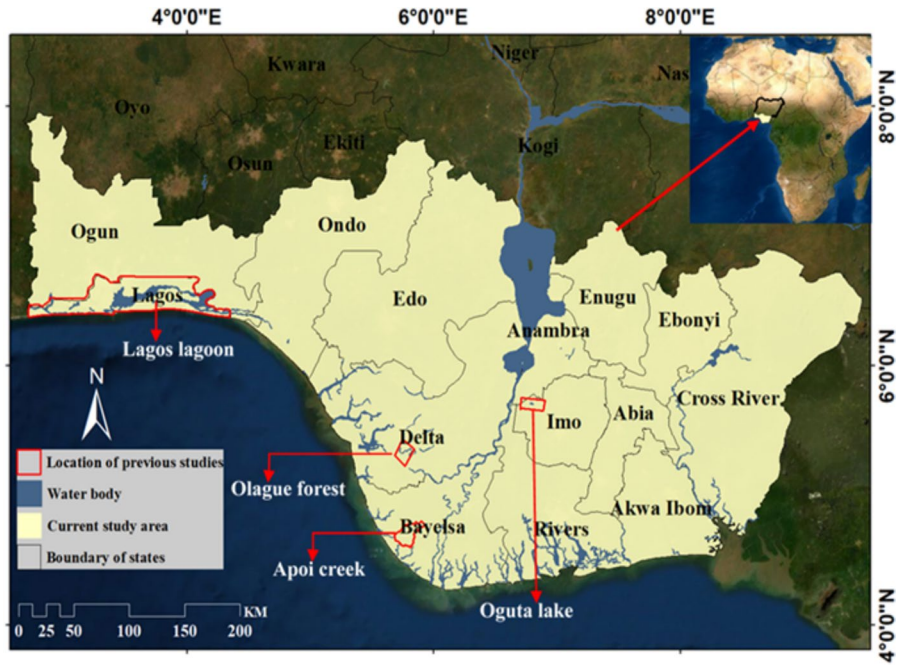

Fig. 1 The study region: **a** Location of the study area using the standard government classification of southern Nigeria, and the locations used in previous studies referred to in the main text: Lagos lagoon (Taiwo & Areola 2009), Olague forest, Apoi creek and Oguta lake (Ayanlade & Proske 2016)

particular can aid classification of dynamic wetlands and their separation from other ecosystems (Mahdianpari et al. 2018; Ozesmi & Bauer 2002). Many wetlands have seasonal characteristics based on changes in water level and vegetation that can assist their detection using remote sensing. For example, marshes experience drying of vegetation and a decrease in water level during the dry season or low tide periods (Murray-Hudson et al. 2006). This can be observed using optical images from a decrease in the reflectivity in the near infrared and a slight increase in reflectivity to the red band due to suspended particles settling out at low water levels (Murray-Hudson et al. 2015).

The increasing availability of open access satellite data, and the growth of advanced machine learning tools integrated with robust cloud computing resources has recently made multi-temporal datasets more accessible (Mahdianpari et al. 2018). The majority of previous studies have used multi-temporal Landsat imagery to classify wetlands both with unsupervised classification algorithms (e.g., K-means and ISODATA; Mwita et al. 2012; Ramsey & Laine 1997) and with supervised classification schemes (Bwangoy et al. 2010; Wright & Gallant 2007), However, it is now possible to supplement this with Synthetic Aperture Radar (SAR) C-band multi polarization radar to discriminate between wetland types (Baghdadi et al. 2001), with cross polarization (HV, VH) providing better discrimination between some wetland classes. Combining multiple optical and SAR indices to classify different wetland types has great potential for wetland classification (Kaplan et al. 2019; Mahdavi et al. 2018; Salehi et al. 2019), however, such approaches have not yet been applied to the wetlands of southern Nigeria. As the only wetland maps that currently span this entire globally important region have pixel sizes of 250 m and 1 km (Gumbricht et al. 2017; Lehner & Döll 2004), there is a need for updated datasets that can be met by the combination of optical and radar satellite data. There are limited attempts to map wetlands using remote sensing across certain parts of Africa. Amongst the few studies we include that of Landmann et al. (2010) were wetlands in western Burkina Faso and southern Mali (in West Africa) were mapped using spectral indices from MODIS and topographic features from SRTM. Mwita et al. (2012) map small scale wetlands in Tanzania and Kenya (in East Africa) using both optical and microwave data employing the decision tree classification techniques.

Here, we map for the first time, the extent of wetlands and categorize the different wetland types for the whole of southern Nigeria (147,094 km^2) at a 10 m resolution, leveraging the open access SAR and optical images acquired from Sentinel-1 and Sentinel-2 and exploiting cloud computing through Google Earth Engine (GEE). Our primary aim is to provide knowledge of wetland extent and character that is needed to support both conservation efforts and land surface climate models. We anticipated that higher resolution wetland mapping would capture smaller patches of wetland than previously documented in regional or global datasets and that this would be dominantly associated with areas near major cities,

Materials and methods

Our approach to mapping the wetlands of southern Nigeria involves the integration of indices from both optical and radar imagery (Fig. 2), and classification of imagery using the implementation of the Random Forest (RF) algorithm in Google Earth Engine (Gorelick et al. 2017). We use seasonal composite images in order to (a) maximise the number of cloud-free pixels and (b) incorporate the seasonal variations in wetland characteristics into our classification (Sects. "Data selection"). We selected the most effective variables for classification in southern Nigeria using an estimation of relative importance (Sect. "Random Forest classification and feature selection"). This required the compilation of a new dataset of 1500 wetland and non-wetland control points for training and validation (Sect. "Compilation of control point data", Supplementary Information).

Class definitions

Wetlands can be classified on the basis of hydrology, soil type and vegetation. They include marshes (freshwater or saline waterlogged land areas that are periodically flooded, dominated by herbaceous plants), swamps (mineral soil wetlands dominated by trees with seasonal flooding), bogs (rain-fed peatlands, which can be with or without trees) and fens (groundwater-fed peatlands, which can be with or without trees) (Mitsch & Gosselink, 2015). In this

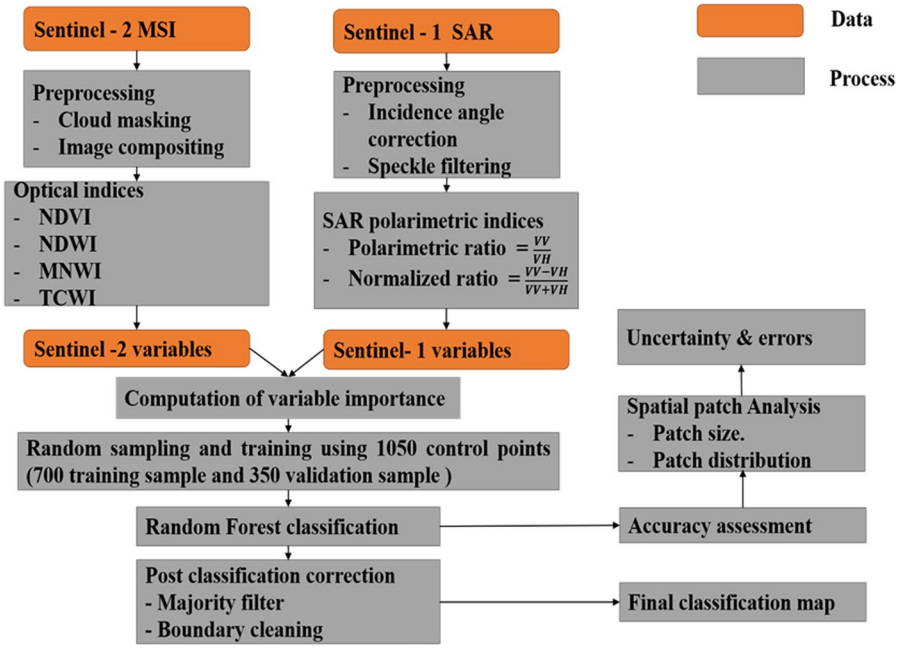

Fig. 2 Methodological approach for mapping and characterization of southern Nigerian wetlands. The technique used a seasonal composite from Sentinel-2 optical imagery and Sentinel-1 radar for 2018

study, we consider swamps, marshes, shallow water (including human-made wetlands and lakes) and the swamp subtype of mangroves (coastal, characterised by salt-tolerant trees and shrubs), and attempt to distinguish between these categories in our mapping. The presence of peatlands (fens) across the southern region of Nigeria has been suggested by other mapping studies (e.g., Center for International Forestry Research (CIFOR), 2016). The Nigerian government, however, suggested that the areas mapped by CIFOR as peatland are more likely to be mangrove/swamps (FREL, 2019). One potential source of confusion is that tropical 'peat swamps' are often referred to in the literature as there is a lack of an agreed tropical peatland classification system. Some swamps can have organic peat deposits while others may have a mineral substrate. To avoid confusion, we strictly classify swamps for our control points as tree-dominated mineral soil wetland systems which may have minimal peat cover. Given this definition, peatland and swamp may in some cases still have similar Earth Observation signatures but would not be confused if ground-truthed.

Data selection

As the characteristics of wetland remote sensing signature varies between seasons, we use composite image for both optical and radar imagery. The southern part of Nigeria experiences a tropical climate with a well-defined wet and dry season. Southern Nigeria is covered by dense cloud during rainy seasons, so we use an initial selection criterion of cloud fraction $< 20\%$ for each of 345 Sentinel-2 images from 2018 and apply a cloud mask to remove cloud and cirrus-cover (using the quality assurance bands available through GEE) before formation of a composite images (Fig. 2). These are constructed from the median value for each pixel in 345 Sentinel-2 images acquired between January and November 2018 and are dominated by dry season (January to March) values. We use blue (0.496 µm, band 2), green (0.560 µm band 3), red (0.665 µm, band 4), and near infrared (NIR, 0.835 µm, band 8), shortwave infrared 1 (SWIR1 1.613 µm, band 11) and short-wave infrared 2 (SWIR2 2.202 µm, band 12) bands to derive optical indices used for classification: Normalized Differential Vegetation Index (NDVI, Chatziantoniou et al. 2017; Dong et al. 2014; Kaplan & Avdan 2017; Xing et al. 2018;Mahdianpari et al. 2018), Normalized Differential Water Index (NDWI, Chatziantoniou et al. 2017; Kaplan & Avdan 2017; Mahdianpari et al. 2018; Xing et al. 2018), Modified Normalized Differential Water Indices (MNDWI, Ashraf & Nawaz 2015; Chen et al. 2013; Ogilvie et al. 2015)

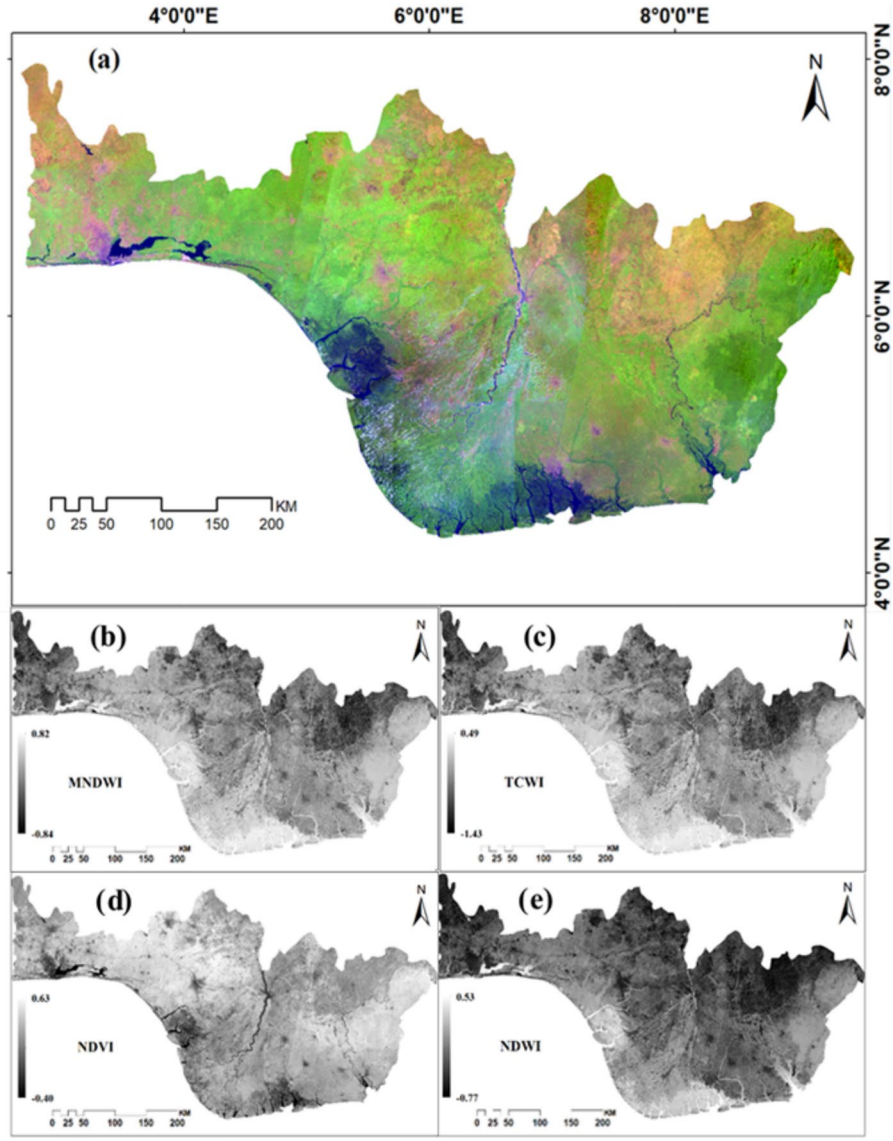

Fig. 3 The Sentinel 2 composite and derived indices for Jan-Dec 2018 used for wetland classification in this study: **a** RGB composite images, red (band 11), blue (band 8), green (band 2), **b** MNDWI, **c** TCWI, **d** NDVI, **e** NDWI. The green shade in the RGB image results from reflection of vegetation, the dark blue shade represent reflection from water bodies, while urban settlement surfaces are shown in purple shade, and the lighter brown shade represents cultivated surfaces. For the indices (**b–e**) lighter gray shade indicates higher moisture and or vegetation value while a darker shade indicates lower values

and Tasseled Cap Wetness Index (TCWI, Tana et al. 2013; Xing et al. 2018) (Fig. 3b–e).

Since SAR backscatter is unaffected by cloud cover, we are able to incorporate information from dry (January–March) and wet seasons (April–July and September–November) into our classification scheme. Differences between flooded and unflooded periods are particularly strong since radar reflected by a water layer and backscattered by a double-bounce from ground and tree trunk creates contrast between the flooded and non-flooded terrain (Bwangoy et al. 2010; Moser et al. 2016). We constructed dry and wet season composites that select the median backscatter value for each pixel, shown in Fig. 4b and c as RGB images where dry season (January–March), wet season (April–July) and end of the wet season (September–November) are the red, blue and green channels, respectively.

We use the Ground Range Detected interferometric wide-swath Sentinel-1 images in ascending orbit from 2018 available through GEE, which are projected onto a regular 10 m grid. Dual VV/VH polarisation imagery was available at an average acquisition interval of 12 days over southern Nigeria. VV polarization (vertically transmitted, vertically

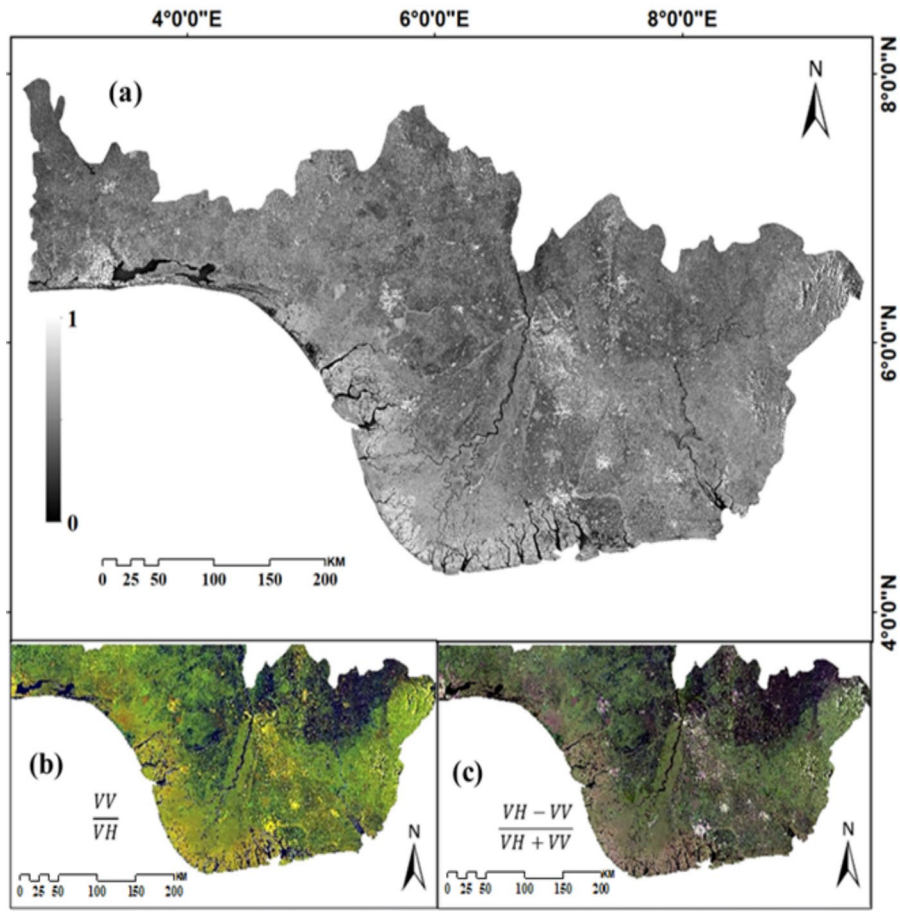

Fig. 4 Extracted features from Sentinel 1 composite: **a** annual composite of VV and VH polarization; **b** seasonal composite images for Jan–Dec 2018 producing a ratio polarized image; **c** seasonal composite images for Jan–Dec 2018 producing a normalized polarized ratio image. The dry season (January–March), wet season (April–July) and end of wet season (September–November) composites were inserted into the red, green and blue channels respectively. The bright yellow shade in (**b**) and bright white in (**c**) shows high backscatter from urban areas in the red and green channels. The dark blue and black shade are the result of low backscatter from cultivated areas and water features

received backscatter) is sensitive to surface roughness and soil moisture and can discriminate flooded from non-flooded vegetation (Mahdianpari et al. 2018). It also produces distinctive returns for herbaceous wetlands with low or sparsely vegetated areas especially in the early growth stages before canopy closure (Baghdadi et al. 2001). VH (vertically transmitted, horizontally received backscatter) known as cross polarization produces signals affected by volume scattering within the vegetation canopy and it is very sensitive to vegetation structures (Steele-Dunne et al. 2017). We corrected for incidence angle (Hird et al. 2017) and reduced radar speckle using an adaptive sigma Lee filter on the GEE platform. We calculated the normalized difference and ratio features for each image as: Ndiff $= \frac{VH-VV}{VH+VV}$ and Nratio $= \frac{VV}{VH}$, where VH is a vertically transmitted, horizontally received SAR backscatter σ^0 from the Sentinel-1 sensor, while VV is vertically transmitted and received SAR backscatter signal (Hird et al. 2017).

Compilation of control point data

We compiled information about the location and characteristics of wetlands in southern Nigeria from multiple sources. Our reference data were obtained from the Food and Agriculture Organization (FAO) global dryland assessment (Bastin et al. 2017), Ramsar Sites database (1971), other organization reports, journals, and academic theses (both PhD and MSc) (see Supplementary Information). The FAO reference points were compared with control sites from Ramsar and other studies, then verified by visual interpretation of Digital Globe very high spatial resolution images (< 1 m pixels) made available for visualization through Google Earth. Our database comprises a total of 1500 sample points for wetland and non-wetland locations. The reference data were grouped into four

wetland types which include swamp (205 points), mangrove (214 points), marsh (121 points), shallow water (184 points) and four non-wetland types grouped into deep water (194 points), urban/bareland (206 points), cultivated land (180 points), and forest (196 points) categories. The photo-interpreted database consists of both wetland and non-wetland cover classes with many subtypes, while only wetland control points were acquired from other studies.

Random Forest classification and feature selection

RF is a non-parametric classifier (i.e., it does not make strong assumptions about the form of the mapping function), comprised of a collection of tree classifiers, and can handle high dimensional remote sensing data (Belgiu & Dra 2016). RF classification involves assigning a label to each pixel based on the majority vote of 'trees'. The 'trees' are grown a node which is spilt using a random selection of the subset input variables, which reduces overfitting and yields a more robust classification than other classifiers (Breiman 2001). In the RF algorithm, we need to specify the parameters in order to produce the forest trees: the number of decision trees to be generated (Ntree); and the number of variables to be selected and tested for the best split when growing the trees (Mtry). The parameter Ntree was assessed for the values of 100 – 600: a value of 500 was selected as error rates for all classification models were constant beyond this point. We tested the importance of sixteen variables (Band 2, Band 3, Band 4, Band 6, Band 7, Band 8, Band 11, Band 12, NDWI, NDVI, MNDWI, TCWI, $\frac{VH-VV}{VH+VV}$, $\frac{VV}{VH}$ (wet and dry)), as input channels for the RF classification. We then selected six input variables that were most important for classification accuracy (see Sect. "Random Forest classification and feature selection"). A total of 900 training points spanning different landcover classes were used to train the RF classifier on the GEE platform. All classifications were based on the same training data. The remaining 600 control points were held back for validation (e.g., Liu et al. 2018). We divided the control points between training and validation data to ensure a spread between landcover classes, and otherwise to make their spatial distribution as even as possible across southern Nigeria. The classification was carried out with each index separately, before selecting the best combination to produce a final wetland map. We classified eight different landcover classes: mangrove, swamp, marsh, shallow water, forest, cultivated land, deep water, built-up/bare land. When selecting input variables used for our final RF classification, we assessed each of the optical and SAR indices for (1) the predictive power of each individual variable (Fig. 5) and (2) the ability to distinguish between wetland classes.

We examine the significance of each input variable by calculating variable importance after training the RF classifier. The importance of a variable in this RF model is assessed using the total decrease in impurity across all trees in the forest for a specific choice of variable to split a node, where impurity refers to the probability of a classification being wrong if it were assigned according only to the distribution of classes in the data. The numerical values for importance assigned to each variable is the sum of the reduction in error of the splitting variable accumulated over the entire tree. Higher variable importance means that the variable played a significant role in the classification, while a low importance means only limited added value by that variable. Figure 5 illustrates the input variables and their corresponding importance for discriminating wetland classes.

As shown above, all the extracted variables from the Sentinel-1 seasonal composite appear to have higher predictive power than the optical indices except for the MNDWI and TCWI. With regards to variables extracted from the Sentinel-2 composite, the optical indices tend to possess higher significance when compared with the individual bands. Among the indices, MNDWI and TCWI have more information available for wetland cover prediction. The most important variables (MNDWI, TCWI, (VH−VV/VH+VV, VV/VH (wet and dry)) from Sentinel-1 and Sentinel-2 were selected for our final classification. However, each variable may have different strength in identifying a particular landcover class regardless of their relative importance. We further perform classifiction on individual variable to optimize our selection of combined model for the final classification map.

Wetland patch analysis

We calculate the number of patches and their individual sizes for each wetland class. The average continuous patch size for each wetland class was

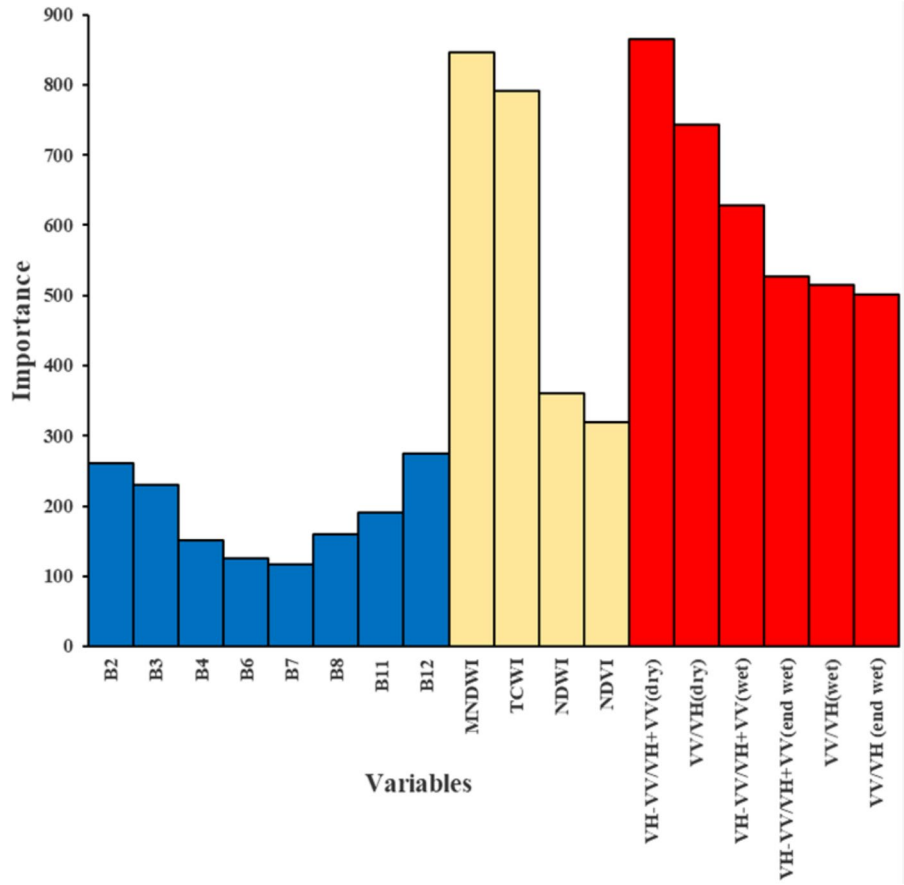

Fig. 5 The importance of each extracted Sentinel-1 and Sentinel-2 features using the training dataset for Random forest classification. The importance of the variable is the sum of decrease impurity each time the variable is selected to be split at the node for the entire trees in the forest and is unitless. The blue bars illustrate the importance of the optical bands, the light yellow shows optical indices and SAR polarimetric indices is represented by red bars

also calculated using the total count of connected pixels for continuous patches, which we define as pixels that share face boundaries. Here, we consider patches where the number of pixels is greater than 1000 (patch size > 1000 pixel) as continuous patches. The area of each individual patch was calculated by multiplying each patch size with the pixel area (10 m^2). The patch size is equivalent to the total number pixels in a patch while the patch area is the patch size x pixel area ($10m^2$). We use:

$$Pch_{avg} = \sum_{j}^{n} \frac{Pch_{cont}}{Pch_{n}}$$

where Pch_{avg} is the average continuous patch for each wetland class in a particular climate zone, Pch_{cont} is the sum of the pixels of continuous patches (for patch size > 1000 pixel) in each class, whereas Pch_n is the total number of continuous patches for each wetland class.

Results

Our final map (Fig. 6) has a pixel size of 10 m and shows how wetlands are distributed in southern Nigeria, broadly consistent with global datasets at low resolution, but quite different when studied in detail at high resolution. We capture wetlands of < 1 km^2 that were omitted from global datasets and therefore provide much needed additional data on wetland coverage. The result of our classification shows high accuracy with 2% uncertainty. We have

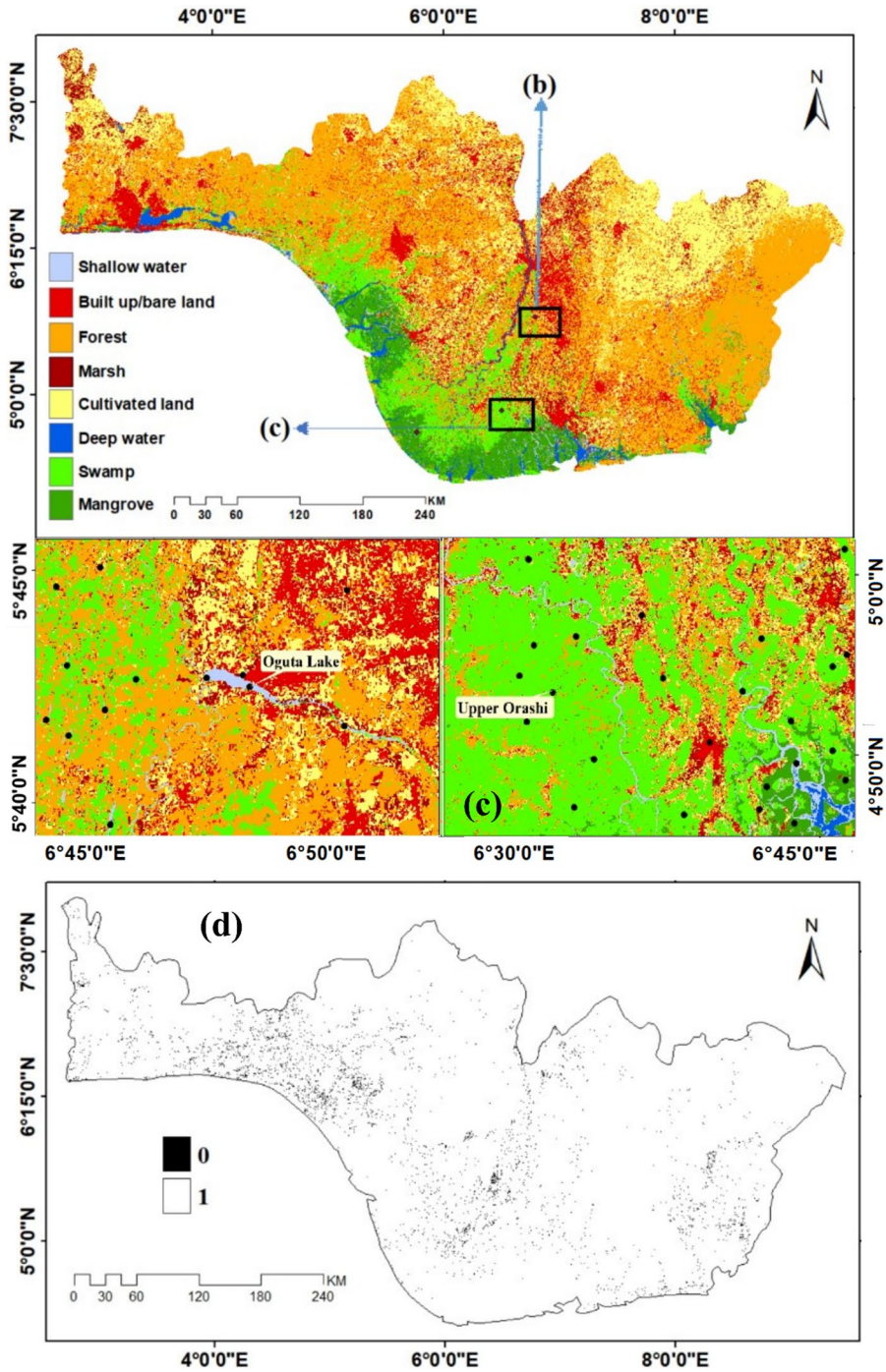

Fig. 6 Final land cover map of southern Nigeria for 2018 obtained from RF classification of indices derived from Sentinel-2 optical data and Sentinel-1 SAR data (**a**), with inset (**b**) showing Oguta Lake and inset (**c**) showing Upper Orashi forest, both being examples of Ramsar wetlands while (**d**) displays the spatial distribution of uncertainty where the value 1 in white shade shows matching landcover class and the value 0 in black shade indicates a mismatch class from the comparison of a map produced using the entire control point dataset with a map produced from a randomly selected subset (70%) of control points

most confidence in our classification of swamp and shallow water, relative to mangrove or marsh.

Classification validation

The results of RF classifications for each index and for our preferred combination of indices (MNDWI, TCWI, (VH−VV/VH+VV, VV/VH (wet and

Table 1 Overall accuracies and Kappa coefficients obtained from classification of wetland versus non-wetland in this study

Indices	Overall accuracy (%)	Kappa coefficient
NDVI	73.10	0.68
NDWI	77.16	0.72
MNDWI	83.78	0.82
TCWI	83.74	0.79
$\frac{VH-VV}{VH+VV}$(wet and dry)	85.14	0.83
$\frac{VV}{VH}$(wet and dry)	74.30	0.72
MNDWI + TCWI+$\frac{VH-VV}{VH+VV}$ + $\frac{VV}{VH}$	88.40	0.85

Perfect classification of control points would yield a Kappa value of 1. S1 + S2 represents our preferred combination of MNDWI and TCWI with the SAR polarimetric indices

dry)) were evaluated using one third (600) of the total control points spatially selected from each class on a random basis. The overall accuracy describes the effectiveness of the overall classification, which can be determined by dividing the sum of correctly classified sample by the total referenced sample (Table 1). The producer's accuracy shows how well the referenced sample is represented in the classified map, while the user′s accuracy indicates the chances that a classified pixel of an individual landcover actually represent the same category on ground (Table 2). The agreement, beyond chance, of a classification and the real land cover can be described by the Kappa coefficient (e.g., Ayanlade & Proske 2016). The Kappa coefficient is more useful than the overall accuracy as it provides a measure of how the classification performs in comparison to the probability of randomly assigning pixels to their correct categories. With the exception of NDVI, the classification results using spectral indices from optical imagery were more accurate than those from SAR imagery alone (Table 1). However, the integration of the SAR normalized difference and ratio images with MNDWI and TCWI yield the highest accuracy. We attribute this to the improvement in accuracy of the identification of marsh, swamp and mangrove classes due to the information about vegetation structure captured by SAR imagery (Fig. 4b and c).

For all landcover classes, classification using a combination of optical and radar data resulted in a higher accuracy than using any of the individual indices in isolation. Our preferred classification (MNDWI + TCWI + VH−VV/VH+VV + VV/VH in Tables 1) performs as well as any other index in its classification of mangroves (214 control sites) and swamps (205 control sites), and better than any other index for classification of marsh (121 control sites). All classes have higher producer′s and user′s accuracies except the marsh with lower users accuracy, which was often misidentified as shallow water or swamp (Table 2). Overall, the classification of wetland classes was less accurate than for non-wetland classes.

The combined use of optical indices (MNDWI and TCWI) and SAR features (VH−VV/VH+VV, VV/VH (wet and dry) resulted in greater accuracy for all the wetland classes than the use of either Sentinel-1

Table 2 Confusion matrix using the set aside validation data (40% of control points)

CLASS	MNG	SWP	FRST	MSH	SHW	BTU	DPW	CTL	Total	User Accuracy
MNG	75	8	1	1	0	0	0	1	86	0.87
SWP	9	69	2	1	0	0	0	1	82	0.84
FRST	1	2	61	2	2	0	0	10	78	0.78
MSH	4	1	0	34	4	0	0	5	48	0.70
SHW	0	0	0	2	67	0	5	0	74	0.90
BTU	0	0	0	0	0	78	0	4	82	0.95
DPW	0	0	0	0	2	0	76	0	78	0.97
CTL	0	0	0	2	0	1	0	69	72	0.95
Total	89	80	64	42	75	79	81	90	600	
Producer Accuracy	0.84	0.86	0.95	0.80	0.89	0.98	0.93	0.76		0.88

The rows are the classification results and the columns are the true class.

MNG Mangrove, *SWP* Swamp, *FRST* Forest, *SHW* Shallow Water, *BTU* Built-up, *DPW* Deep water, *CTL* Cultivated land

or Sentinel-2 imagery in isolation, and so this combination was used to produce our final wetland map.

Our final wetland cover map (Fig. 6a) shows the distribution of all land-cover classes, at 10 m resolution, across the extensive area of southern Nigeria. Both the wetland and non-wetland cover are well delineated with an estimated mapping accuracy of 88%. The detailed inset in Fig. 6b and c shows how shallow water (e.g., Oguta lake, Fig. 6b) and swamp (e.g., Upper Orashi swamp forest) are correctly distinguished from other landcover classes at two Ramsar wetland locations. We make an assessment of the spatial distribution of uncertainty in our wetland map by comparing it to a map produced from a randomly selected subset (70%) of control points with the map produced using the entire dataset (Fig. 6d). On Fig. 6d we show locations where land cover classifications agree for the two maps a value of 1 (white), and those that disagree a value of zero (black). We found that mismatches mostly lie on swamp and marsh landcover classes (Fig. 6d), with fewer found to lie on mangrove and shallow water.

Wetland spatial extent

We estimate that the wetlands of southern Nigeria cover a total area of 29,924 km^2 which is over one fifth of the area of the whole region. The dominant wetland type is swamp which made up 44% of the total wetland area followed by mangrove (31%), marsh (20%) and shallow lakes (5%) (Fig. 7). The vast majority of these wetlands are located in the coastal region of the Niger delta and Lagos. Our estimate of total wetland cover is less than the estimate by Center for International Forestry Research (CIFOR) (31,829 km^2) but larger than GLWD (24,408 km^2) (Fig. 7), mainly resulting from our larger mapped area of mangrove and our identification of fewer marsh wetlands. While the maps look similar when viewed at low resolution, they are quite different in detail (Fig. 7).

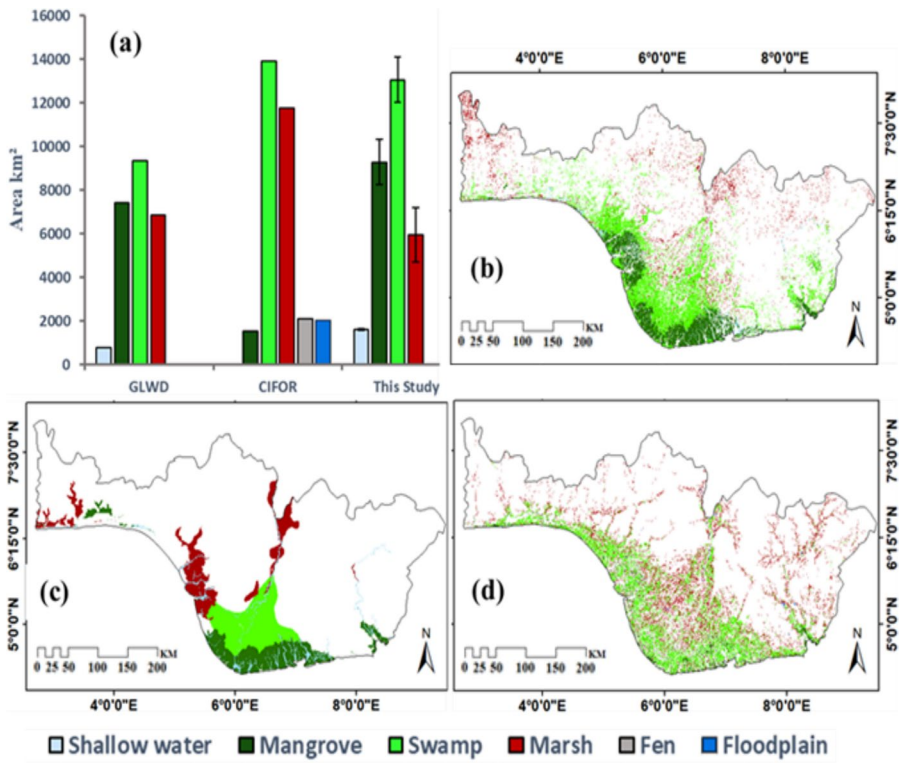

Fig. 7 A comparison of wetland map products for southern Nigeria: **a** areas of different wetland classes in southern Nigeria—error bars show misclassification levels based accuracy achieved for each wetland type in our study; **b** map of southern Nigeria covered by wetlands identified in our study showing only the wetland classes; **c** the Global Lakes and Wetlands Database (GLWD) by Lehner and Döll (2004) and **d** the global wetland database by the Center for International Forestry Research (CIFOR)

Discussion

Wetland extent and fragmentation

We calculated the average continuous patch size for each wetland class using the total pixel count of connected pixels for continuous patches, which we define as pixels that share face boundaries. We found mean continuous wetland patches of 120, 11, 55 and 13 km^2 for mangrove, marsh, swamp, and shallow water respectively. The maximum patch size was 2740, 1530, 160 and 50 km^2 with a standard deviation of 660, 765, 25 and 26 km^2 for these wetland types respectively. Larger patches of wetland are found along the coastal areas while smaller fragments are mostly located around urban areas suggesting a role for anthropogenic fragmentation of wetlands. Mangroves tended to be located in zones with lower population density. There were a large number of small wetland fragments, mostly of single pixel patches, especially for the marsh class (Fig. 8). These smaller patches were distributed across the map but had higher uncertainty relative to larger patches. Understanding wetland fragmentation and its impacts on biodiversity and ecosystem services, and the role of both larger and smaller wetland patches in landscapes requires further work, but our dataset provides a starting point for enhanced modelling of such effects.

The extent of wetland in southern Nigeria was found to be larger in our study when compared to some previous studies but was smaller than the estimate by CIFOR (Fig. 7a). This discrepancy could be due to a combination of factors including differences in wetland land cover class definitions (e.g., in CIFOR's global wetland database https://www.cifor.org/global-wetlands/ swamps and bogs are classed as one type of wetland, while many floodplain wetlands appear to be swamps in our wetland map), classification methodology, timeframe (e.g., wetland loss or creation between different studies), data resolution and time of acquisition. For example, more conservative methods used by previous studies based on combining existing maps with other data sources may have resulted in exclusion of a large proportion of the swamp and mangrove that we identify here. Another

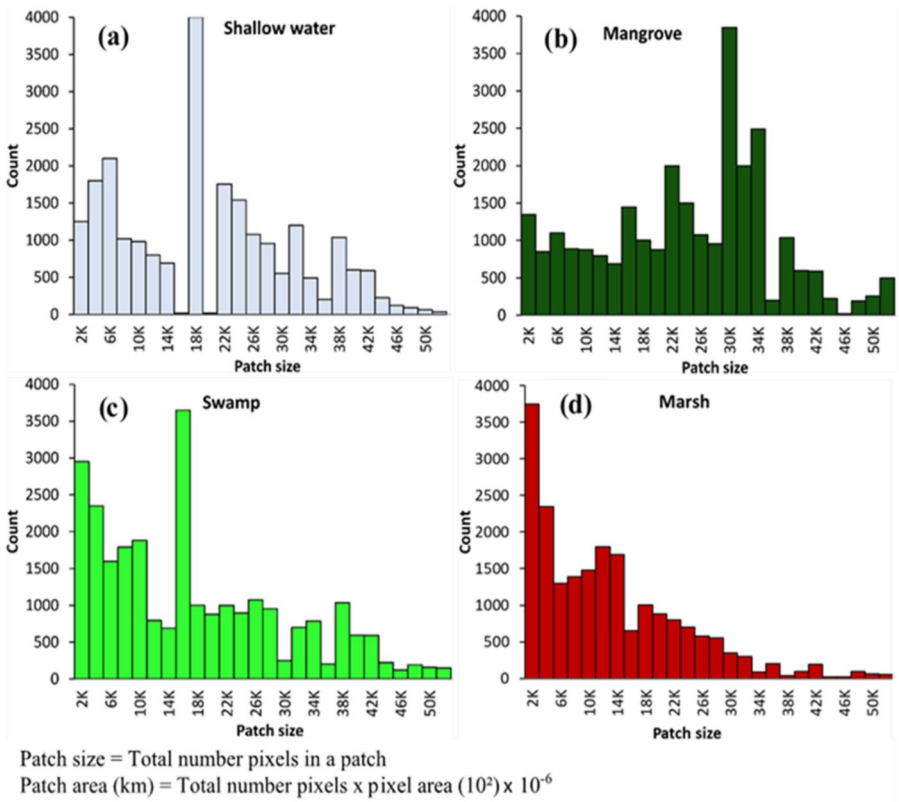

Fig. 8 Distribution of patch size for different wetland classes: **a** shallow water; **b** mangrove; **c** swamp; **d** marsh. The patch size is defined as the number of pixels within a patch, the count is the frequency of patches with number of pixels in each category

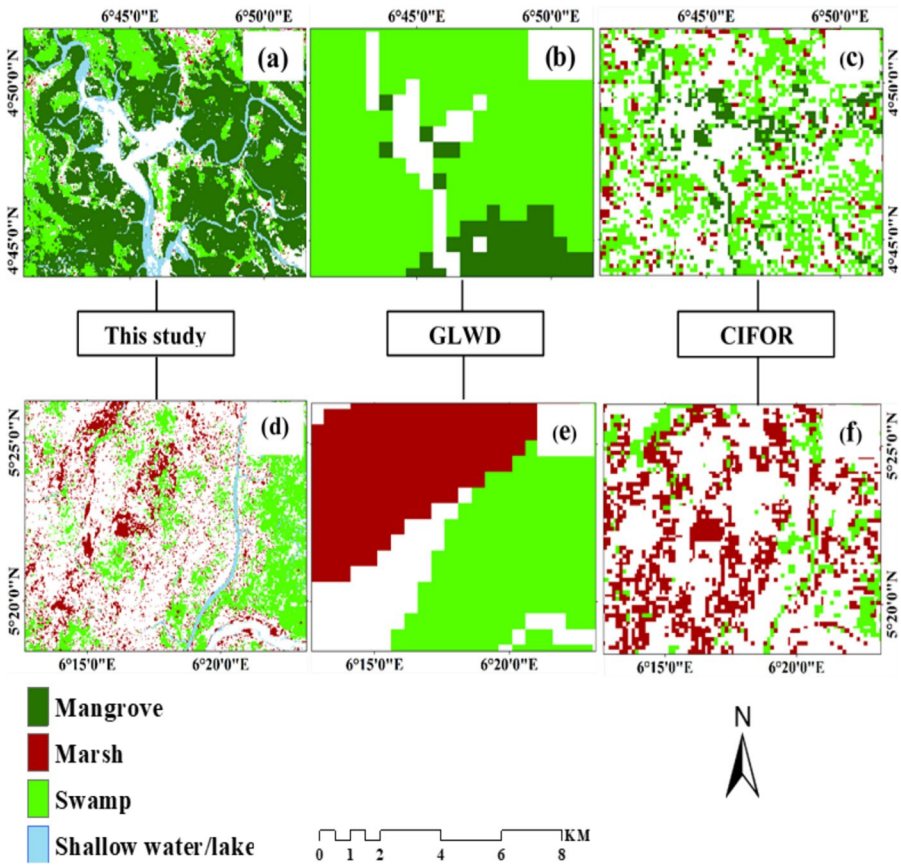

Fig. 9 Comparison, for the same geographical area, between delineated wetland cover in two example locations (first location shown in top row **a–c**, second location shown as bottom row **d–e**): **a** and **d** this study using high resolution Sentinel data (full map shown in Fig. 6a), **b** and **e** GLWD from a combination of low-resolution data, **c** and **f** the global wetland database by the Center for International Forestry Research (CIFOR)

major difference is our use of satellite imagery with higher resolution (10 m pixel size, relative to 1 km for GLWD) which improves our ability to identify small-scale wetlands (see Fig. 9) and aids in discriminating wetland and non-wetland features. Some areas where wetlands have not previously been reported (e.g., around Akampka in Cross Rivers) have been mapped in our study. Some studies have suggested that the GLWD may underestimate wetland extent because of low resolution input data (Gumbricht et al. 2017), so wetlands much smaller than 1 km^2 are missed. About 20% of the wetlands that we identify in our new map have spatial extents of < 1 km^2 (100 pixels). A series of small wetlands may be very important at a landscape scale in terms of water, nutrient and carbon cycling dynamics (Blackwell and Pilgrim, 2011) and so our work indicates how higher resolution wetland mapping may be important for improving regional and global environmental models.

Sources of uncertainty

The most important sources of uncertainty in this study come from (1) the subtlety of the differences in remote sensing signals between some wetland classes, and (2) the distribution and characteristics of the control sites used as the reference for different land-cover types. Specifically, we expect uncertainties to be introduced by both a lower number of control sites for marshes and similarities in the remote sensing expression of marshes vs. mangroves, especially at 1610 and 2190 nm. We assess our uncertainties by comparing classifications made using the entire control point dataset with those produced using only a subset of control points selected at random for each wetland class (see Fig. 6d). The mismatched pixels from each class were multiplied with the pixel area to obtain the mismatched area for each class. Swamp, with a total area of 13,000 km^2 had the highest uncertainty of 250 km^2 followed by marsh (area of 6000 km^2) with uncertainty of 123 km^2. Lower uncertainty

was estimated for mangrove (9000 km^2) at 72 km^2 and shallow water (1616 km^2) with 14 km^2. While this approach gives some indication of the uncertainties associated with our classification accuracy and limitations in the number of control points, it does not include systematic uncertainties associated with our choice of landcover classes. However, more than 98% of the control points accurately matched the classified land-cover class. Based on control point accuracy values for each wetland type (Table 2) there was a higher error with marshes due to their misinterpretation as mangroves and bare land / settlement features. A higher uncertainty occurred in areas around Ovia (south-west Edo state), northern parts of Ogun state and around Ndokwa in eastern Delta state due to the number of smaller patches of marsh. There were no control points for fen peatlands. However, our analysis suggests that areas mapped by other studies as peatlands (e.g., around Apoi creek forest) (refer to Fig. 1a) in southern Nigeria are swamps (with total of 149 control points), for which we had a high confidence in their classification.

Data limitations

Despite the high accuracy obtained from the classification model, there are some limitations in the dataset that may lead to bias in the model. Using training data from existing wetland locations is affected by ambiguity in definitions of wetland class and variation in the landscape. The basic assumption that training data represent a particular class may not always be absolutely correct as individual training points may belong to other wetland classes. To address this, we characterize the training data based on the class composition and internal variability. We then identify the possible outliers from the distribution of each wetland class and filter them out from the training data. Training data for ephemeral forested wetlands and peatlands such as bogs, fens are missing from our dataset which would have improved our classification.

The imbalance in the size of our training data for the wetland classes may bias classification accuracy, because the model is sensitive to wetland class with larger numbers of training points (in our case [mangrove]). This results in higher accuracy than for wetland classes with small amounts of training data (e.g., marsh).

Users of our wetland map should also consider (1) the limitations of the class definitions appropriate for use with satellite imagery and (2) the differences in accuracy of classification for different classes due to different numbers and spatial distribution of training points. For example, our EO-based classification of [swamps] comprises wetland with a range of characterisitics in terms of vegetation type, water depth and soil composition.

Applicability to different settings

Our novel study adds to a small number of locations around the world where wetlands have been mapped using combined SAR and optical Sentinel 1 and 2 data (e.g., Hird et al. 2017; Mahdianpari et al. 2018; Slagter et al. 2020). However, here we have covered a much larger area at high resolution. The wetlands of southern Nigeria are thought to represent about 19% of West African wetland and 3% of the total wetlands in sub Saharan Africa (Rebelo et al. 2010). Nigerian wetland ecosystems are similar to those in the rest of West Africa, so we expect that similar classification approaches could be adopted for this region. Our methodological approach could be expanded to explore wetland areas across the wider African continent as well as globally. Furthermore, our technique can be used to globally detect changes and connectivity/fragmentation of wetland ecosystem in response to human action such as urbanization. Using data from different seasons is important for mapping and distinguishing between different types of wetland extents. For example, seasonal data has played an important role in identification of shallow water and marshes (Fig. 6a). Seasonal data will be essential for mapping the wetlands in the arid regions of Africa, where wetlands exhibit dramatic seasonal cycles (e.g., the Sebkhel el Kelbia of Tunisia). Challenges of producing high-resolution datasets over large spatial areas can be minimized by employing the SAR polarimetric feature and optical indices which help to distinguish between types of vegetation. Wetland types such as peatlands which were not covered in this study should be mapped using suitable control points to aid classification. There is also a need to incorporate elevation/topographic data and a diverse range of multi-temporal datasets in order to improve the identification of wetlands across different terrain, such as

valley bottom wetlands. This will help to capture the hydrogeomorphological properties of the wetlands.

Conclusions

Our study combined optical indices and SAR polarimetric features to map four wetland types at 10 m resolution across southern Nigeria, filling a gap between existing low spatial resolution global maps and a few very local studies at higher resolution. Using freely available global satellite datasets (Sentinel-1 and 2), we achieve a mapping accuracy of 88% by integrating optical indices and SAR polarimetric features from different seasons using Random Forest classification. We estimate that in 2018 southern Nigeria contained 29,924 km^2 of wetlands with an uncertainty of 460 km^2, covering 20% of the region. We found a large number of small wetland patches, particularly around urban areas, consistent with human action enhancing wetland fragmentation in Southern Nigeria. Given the rapid expansion of population in Nigeria, it is now critical that wetland protection organizations undertake more adequate change detection at high resolution and take action, while modellers can utilise our high resolution land surface data.

Acknowledgements This project was funded by a studentship awarded to SIG under the Petroleum Technology and Development Fund (PTDF) Nigeria. The photo-interpretation dataset was part of the global dryland assessment which was conducted in the region by the Food and Agriculture Organization and the National Space Research and Development Agency of Nigeria. SKE is supported by a NERC Independent Research Fellowship (NE/R015566/1).

Author contributions All authors contributed to data curation, review and editing of the research paper. Conceptualization, methodology, design and analysis were performed by SG, JH and SE. Writing of the original draft of the manuscript was written by SG and all authors commented on previous versions of the manuscript. All authors read and approved the final manuscript.

Funding The sources of funding were mentioned in the Acknowledgements section.

Data availability The 10 m resolution shapefile for the wetland map produced and the ground control data used are all available at the Research Data Leeds repository: https://doi.org/10.5518/1314.

Declarations

Conflict of interest The authors declare no conflict of interests.

Open Access This article is licensed under a Creative Commons Attribution 4.0 International License, which permits use, sharing, adaptation, distribution and reproduction in any medium or format, as long as you give appropriate credit to the original author(s) and the source, provide a link to the Creative Commons licence, and indicate if changes were made. The images or other third party material in this article are included in the article's Creative Commons licence, unless indicated otherwise in a credit line to the material. If material is not included in the article's Creative Commons licence and your intended use is not permitted by statutory regulation or exceeds the permitted use, you will need to obtain permission directly from the copyright holder. To view a copy of this licence, visit http://creativecommons.org/licenses/by/4.0/.

References

Ashraf M, Nawaz R (2015) A comparison of change detection analyses using different band algebras for Baraila wetland with Nasa's multi-temporal Landsat dataset. J Geogr Inf Syst 07(01):1–19. https://doi.org/10.4236/jgis.2015.71001

Ayanlade A, Proske U (2016) Assessing wetland degradation and loss of ecosystem services in the Niger Delta. Nigeria Marine Freshwater Res 67(6):828–836. https://doi.org/10.1071/MF15066

Baghdadi N, Bernier M, Gauthier R, Neeson I (2001) Evaluation of C-band SAR data for wetlands mapping. Int J Remote Sens 22(1):71–88. https://doi.org/10.1080/014311601750038857

Bastin J-F, Berrahmouni N, Grainger A, Maniatis D, Mollicone D, Moore R et al (2017) The extent of forest in dryland biomes. Science 358(6365):635–638. https://doi.org/10.1126/science.aao1309

Belgiu M, Dra L (2016) Random forest in remote sensing: a review of applications and future directions. ISPRS J Photogramm Remote Sens 114:24–31. https://doi.org/10.1016/j.isprsjprs.2016.01.011

Breiman LEO (2001) Random forests. Mach Learn 45:5–32

Bwangoy JRB, Hansen MC, Roy DP, Grandi GD, Justice CO (2010) Wetland mapping in the Congo Basin using optical and radar remotely sensed data and derived topographical indices. Remote Sens Environ 114(1):73–86. https://doi.org/10.1016/j.rse.2009.08.004

Center for International Forestry Research (2016) Global wetland. https://www.cifor.org/global-wetlands

Chatziantoniou A, Petropoulos GP, Psomiadis E (2017) Co-orbital sentinel 1 and 2 for LULC mapping with emphasis on wetlands in a mediterranean setting based on machine learning. Remote Sens 9(12):1259. https://doi.org/10.3390/rs9121259

Chen Y, Huang C, Ticehurst C, Merrin L, Thew P (2013) An evaluation of MODIS daily and 8-day composite products for floodplain and wetland inundation mapping.

Wetlands 33(5):823–835. https://doi.org/10.1007/s13157-013-0439-4
Chidumeje NPO, Lalit K, Subhashni T (2015) The Niger Delta wetland ecosystem: what threatens it and why should we protect it? Afr J Environ Sci Technol 9(5):451–463. https://doi.org/10.5897/AJEST2014.1841
Clark DB, Mercado LM, Sitch S, Jones CD, Gedney N, Best MJ et al (2011) The Joint UK Land Environment Simulator (JULES), model description—part 2: carbon fluxes and vegetation dynamics. Geosci Model Dev 4(3):701–722. https://doi.org/10.5194/gmd-4-701-2011
Dadson SJ, Ashpole I, Harris P, Davies HN, Clark DB, Blyth E, Taylor CM (2010) Wetland inundation dynamics in a model of land surface climate: evaluation in the Niger inland delta region. J Geophys Res Atmos 115(23):1–7. https://doi.org/10.1029/2010JD014474
Dong Z, Wang Z, Liu D, Song K, Li L, Jia M, Ding Z (2014) Mapping wetland areas using landsat-derived NDVI and LSWI: a case study of West Songnen Plain, Northeast China. J Indian Soc Remote Sens 42(3):569–576. https://doi.org/10.1007/s12524-013-0357-1
Fei SX, Shan CUIH, Hua GUOZ (2011) Remote sensing of mangrove wetlands identification. Procedia Environ Sci 10:2287–2293. https://doi.org/10.1016/j.proenv.2011.09.357
Gorelick N, Hancher M, Dixon M, Ilyushchenko S, Thau D, Moore R (2017) Remote sensing of environment Google Earth engine: planetary-scale geospatial analysis for everyone. Remote Sens Environ 202:18–27. https://doi.org/10.1016/j.rse.2017.06.031
Gumbricht T, Roman-Cuesta RM, Verchot L, Herold M, Wittmann F, Householder E et al (2017) An expert system model for mapping tropical wetlands and peatlands reveals South America as the largest contributor. Global Change Biol 23(9):3581–3599. https://doi.org/10.1111/gcb.13689
Guo M, Li J, Sheng C, Xu J, Wu L (2017) A review of wetland remote sensing. Sensors (Switzerland) 17(4):1–36. https://doi.org/10.3390/s17040777
Hassan T, Majid M, Davidson SA, Medugu N (2014) The role of wetlands in mitigating the effect of climate change in Nigeria. Handbook of Climate Change Adaptation. https://doi.org/10.1007/978-3-642-40455-9_109-2
Hird JN, Delancey ER, Mcdermid GJ (2017) Google Earth engine, open-access satellite data, and machine learning in support of large-area probabilistic wetland mapping. Remote Sens 9:1315. https://doi.org/10.3390/rs9121315
Hu S, Niu Z, Chen Y (2017) Global wetland datasets: a review. Wetlands 37(5):807–817. https://doi.org/10.1007/s13157-017-0927-z
Igu NI, Marchant R (2017) Freshwater swamp forest use in the Niger Delta : perception and insights. J for Res 22(1):44–52. https://doi.org/10.1080/13416979.2017.1280887
Junk WJ, An S, Finlayson CM, Gopal B, Květ J, Mitchell SA et al (2013) Current state of knowledge regarding the world's wetlands and their future under global climate change: a synthesis. Aquat Sci 75(1):151–167. https://doi.org/10.1007/s00027-012-0278-z
Kaplan G, Avdan U (2017) Mapping and monitoring wetlands using Sentinel-2 satellite imagery. ISPRS Ann Photogrammetry, Remote Sens Spatial Inf Sci 4:271–277
Kaplan G, Yigit Avdan Z, Avdan U (2019) Mapping and monitoring wetland dynamics using thermal, optical, and SAR remote sensing data. Wetlands Manage Assess Risk Sustain Solutions. https://doi.org/10.5772/intechopen.80264
Klemas V (2011) Remote sensing of wetlands: case studies comparing practical techniques. J Coastal Res 27(3):418–427. https://doi.org/10.2112/JCOASTRES-D-10-00174.1
Kuenzer C, Bluemel A, Gebhardt S, Quoc TV, Dech S (2011) Remote sensing of mangrove ecosystems: a review. Remote Sens 3(5):878–928. https://doi.org/10.3390/rs3050878
Landmann T, Schramm M, Colditz RR, Dietz A, Dech S (2010) Wide area wetland mapping in semi-arid Africa using 250-meter MODIS metrics and topographic variables. Remote Sens 2:1751–1766
Lehner B, Döll P (2004) Global Lakes and Wetlands database GLWD. Wetlands 296(1–4):1–7
Liu Y, Gong W, Hu X, Gong J (2018) Forest type identification with random forest using sentinel-1a, sentinel-2a, multi-temporal Landsat-8 and DEM data. Remote Sens 10(946):1–25. https://doi.org/10.3390/rs10060946
Mahdavi S, Salehi B, Granger J, Amani M, Brisco B, Huang W (2018) Remote sensing for wetland classification: a comprehensive review. GIScience Remote Sens 55(5):623–658. https://doi.org/10.1080/15481603.2017.1419602
Mahdianpari M, Salehi B, Mohammadimanesh F, Homayouni S, Gill E (2018) The first wetland inventory map of newfoundland at a spatial resolution of 10 m using sentinel-1 and sentinel-2 data on the google earth engine cloud computing platform. Remote Sens 11:43. https://doi.org/10.3390/rs11010043
Mitsch WJ, Gosselink JG (2015) Wetlands Fifth Edition. Wiley 5:721. https://doi.org/10.1017/CBO9781107415324.004
Moser L, Schmitt A, Wendleder A, Roth A (2016) Monitoring of the Lac Bam wetland extent using dual-polarized X-band SAR data. Remote Sens 8:302. https://doi.org/10.3390/rs8040302
Murray-Hudson M, Wolski P, Ringrose S (2006) Scenarios of the impact of local and upstream changes in climate and water use on hydro-ecology in the Okavango Delta. Botswana J Hydrol 331(1–2):73–84. https://doi.org/10.1016/j.jhydrol.2006.04.041
Murray-Hudson M, Wolski P, Cassidy L, Brown MT, Thito K, Kashe K, Mosimanyana E (2015) Remote sensing-derived hydroperiod as a predictor of floodplain vegetation composition. Wetlands Ecol Manage 23(4):603–616. https://doi.org/10.1007/s11273-014-9340-z
Mwita E, Menz G, Misana S, Becker M, Kisanga D, Boehme B (2012) Mapping small wetlands of Kenya and Tanzania using remote sensing techniques. Int J Appl Earth Obs Geoinf 21(1):173–183. https://doi.org/10.1016/j.jag.2012.08.010
National Forest Reference Emission Level (FREL) for the Federal Republic of Nigeria (2019), pp 1–5
Obiefuna JN, Nwilo PC, Atagbaza AO, Okolie CJ (2013) Land cover dynamics associated with the spatial changes in the Wetlands of Lagos/Lekki Lagoon system of Lagos. Nigeria J Coastal Res 288(3):671–679. https://doi.org/10.2112/JCOASTRES-D-12-00038.1
Ogilvie A, Belaud G, Delenne C, Bailly JS, Bader JC, Oleksiak A et al (2015) Decadal monitoring of the Niger

Inner Delta flood dynamics using MODIS optical data. J. Hydrol 523:368–383. https://doi.org/10.1016/j.jhydrol.2015.01.036

Olalekan EI (2014) Wetland resources of Nigeria: case study of the Hadejia-Nguru wetlands. Poult Fish Wildl Sci. https://doi.org/10.4172/2375-446X.1000123

Ozesmi SL, Bauer ME (2002) Satellite remote sensing of wetlands. Wetlands Ecol Manage 10(5):381–402. https://doi.org/10.1023/A:1020908432489

Ramsey EW, Laine SC (1997) Comparison of Landsat thematic mapper and high resolution photography to identify change in complex coastal wetlands. J Coastal Res 13(2):281–292

Rebelo LM, McCartney MP, Finlayson CM (2010) Wetlands of Sub-Saharan Africa: distribution and contribution of agriculture to livelihoods. Wetlands Ecol Manage 18(5):557–572. https://doi.org/10.1007/s11273-009-9142-x

Salehi B, Mahdianpari M, Amani M, Manesh F, Granger J, Mahdavi S, Brisco B (2019) A collection of novel algorithms for wetland classification with SAR and optical data. Wetlands Manage Assess Risk Sustain Solutions. https://doi.org/10.5772/intechopen.80688

Slagter B, Tsendbazar N-E, Vollrath A, Reiche J (2020) Mapping wetland characteristics using temporally dense Sentinel-1 and Sentinel-2 data: a case study in the St Lucia wetlands, South Africa. Int J Appl Earth Observ Geoinf 86:102009. https://doi.org/10.1016/j.jag.2019.102009

Steele-Dunne SC, McNairn H, Monsivais-Huertero A, Member S (2017) Radar remote sensing of agricultural canopies: a review. IEEE J Select Topics Appl Earth Observ Remote Sens 10(2):2249–2273. https://doi.org/10.1109/JSTARS.2016.2639043

Taiwo OJ, Areola O (2009) A spatial temporal analysis of wetland losses in the Lagos coastal region, Southwestern Nigeria, using multi-date satellite imagery. Int Geosci Remote Sens Symp (IGARSS) 3:928–930. https://doi.org/10.1109/IGARSS.2009.5417924

Tana G, Letu H, Cheng Z, Tateishi R (2013) Wetlands mapping in north America by decision rule classification using MODIS and ancillary data. IEEE J Select Topics Appl Earth Observ Remote Sens 6(6):2391–2401. https://doi.org/10.1109/JSTARS.2013.2249499

The Ramsar Convention Secretariat (1971) The Ramsar Sites Criteria. [ebook] Ramsar, Iran: Ramsar Sites database

Uloacha N, Okeke I (2004) Implications of wetlands degradation for water resources management. GeoJournal 61(2):151–154

Wilen ABO, Bates MK (1995) The US fish and wildlife service's National wetlands inventory project. Vegetatio 118(1):153–169

Wright C, Gallant A (2007) Improved wetland remote sensing in Yellowstone National Park using classification trees to combine TM imagery and ancillary environmental data. Remote Sens Environ 107(4):582–605. https://doi.org/10.1016/j.rse.2006.10.019

Xing L, Tang X, Wang H, Fan W, Gao X (2018) Mapping Wetlands of Dongting Lake in China Using Landsat and sentinel-1 time series at 30M. Int Remote Sens Spatial Inf Sci 12:1971–1976

Xu J, Morris PJ, Liu J, Holden J (2018) PEATMAP: Refining estimates of global peatland distribution based on a meta-analysis. CATENA 160:134–140. https://doi.org/10.1016/j.catena.2017.09.010

Ohimain, E. (1996). Environmental impacts of dredging in the Niger Delta. *Habitat*, 9–19.

Publisher's Note Springer Nature remains neutral with regard to jurisdictional claims in published maps and institutional affiliations.